THE JOURNAL OF BIOLOGICAL CHEMISTRY VOL. 285, NO. 42, pp. 32126–32140, October 15, 2010

Changes in Accessibility of Cytoplasmic Substances to the Pore Associated with Activation of the Cystic Fibrosis Transmembrane Conductance Regulator Chloride Channel*[S]

Received for publication, February 11, 2010, and in revised form, July 29, 2010 Published, JBC Papers in Press, July 30, 2010, DOI 10.1074/jbc.M110.113332

Yassine El Hiani and Paul Linsdell[1]

From the Department of Physiology and Biophysics, Dalhousie University, Halifax, Nova Scotia B3H 1X5, Canada

Opening of the cystic fibrosis transmembrane conductance regulator Cl^- channel is dependent both on phosphorylation and on ATP binding and hydrolysis. However, the mechanisms by which these cytoplasmic regulatory factors open the Cl^- channel pore are not known. We have used patch clamp recording to investigate the accessibility of cytoplasmically applied cysteine-reactive reagents to cysteines introduced along the length of the pore-lining sixth transmembrane region (TM6) of a cysteine-less variant of cystic fibrosis transmembrane conductance regulator. We find that methanethiosulfonate (MTS) reagents modify irreversibly cysteines substituted for TM6 residues Phe-337, Thr-338, Ser-341, Ile-344, Val-345, Met-348, Ala-349, Arg-352, and Gln-353 when applied to the cytoplasmic side of open channels. However, the apparent rate of modification by internal [2-sulfonatoethyl] methanethiosulfonate (MTSES), a negatively charged MTS reagent, is dependent on the activation state of the channels. In particular, cysteines introduced far along the axis of TM6 from the inside (T338C, S341C, I344C) showed no evidence of significant modification even after prolonged pretreatment of non-activated channels with internal MTSES. In contrast, cysteines introduced closer to the inside of TM6 (V345C, M348C) were readily modified in both activated and non-activated channels. Access of a permeant anion, $Au(CN)_2^-$, to T338C was similarly dependent upon channel activation state. The pattern of MTS modification we observe allows us to designate different pore-lining amino acid side chains to distinct functional regions of the channel pore. One logical interpretation of these findings is that cytoplasmic access to residues at the narrowest region of the pore changes concomitant with activation.

Cystic fibrosis is caused by genetic mutations that lead, via a variety of molecular mechanisms, to loss of function of the cystic fibrosis transmembrane conductance regulator (CFTR)[2] (1). CFTR is a member of a large group of membrane ATPases, the ATP binding cassette transporter family, but is unique within this large family of proteins in acting as an ion channel (2). As with other ATP binding cassette proteins, CFTR has a modular architecture consisting of two transmembrane domains (TMDs), each possessing six membrane-spanning α-helices, and two cytoplasmic nucleotide binding domains (NBDs). CFTR also has a unique cytoplasmic domain, the R domain, that links its two homologous TMD-NBD halves.

The physiological role of CFTR is to form a protein kinase A (PKA)-regulated anion conductance across the apical membrane of many different epithelial cells (3). Although CFTR is commonly referred to as a Cl^- channel, permeation of HCO_3^- (4–6), glutathione (7), and SCN^- (8) may also be physiologically relevant. The structure of the channel pore through which these anions cross the membrane is unknown, although transmembrane (TM) α-helices TM1, -5, -6, -11, and -12 are all thought to make some contribution to the lining of the pore (9–13). Regulation of channel activity is via phosphorylation and dephosphorylation of the R domain, with PKA-mediated phosphorylation being an absolute prerequisite for channel opening (2). Once activated by phosphorylation, channel opening and closing is controlled by ATP binding and hydrolysis by a heterodimer of the two NBDs (2, 14–16). It is presumed that a "gate" located somewhere in the membrane-spanning pore regulates Cl^- flow and that this gate is in turn controlled by the NBDs (2, 14, 15). However, the identity or location of such a gate has never been reported.

Among the TMs, TM6 is well known to play a key role in forming the CFTR pore and determining its functional properties (9, 10). To gain some information on conformational changes occurring in the CFTR pore, we have, therefore, studied the accessibility of residues in TM6 to substances applied from the cytoplasmic side of the membrane. We find that cysteine-reactive reagents can penetrate deep into the pore of open channels to modify cysteine side chains introduced along the axis of TM6. In contrast, only cysteines located relatively close to the intracellular end of TM6 can apparently be modified before channel activation. Based on these findings, we propose a model in which localized structural rearrangements in TM6 alter the accessibility of cytoplasmic substances to the pore concomitant with channel activation. We speculate that such rearrangements could provide a mechanism by which pore transport function is regulated.

EXPERIMENTAL PROCEDURES

Experiments were carried out on baby hamster kidney cells transiently transfected with human CFTR. In this study we have

* This work was supported by the Canadian Institutes of Health Research.
[S] The on-line version of this article (available at http://www.jbc.org) contains supplemental Figs. S1–S3.
[1] To whom correspondence should be addressed. Tel.: 902-494-2265; Fax: 902 494 1685; E-mail: paul.linsdell@dal.ca.
[2] The abbreviations used are: CFTR, cystic fibrosis transmembrane conductance regulator; TM, transmembrane α-helix; TMD, transmembrane domain; MTS, methanethiosulfonate; MTSES, [2-sulfonatoethyl] MTS; MTSET, [2-(trimethylammonium)ethyl] MTS; NBD, nucleotide binding domain; TES, *N*-tris(hydroxymethyl)methyl-2-aminoethanesulfonate.

used a human CFTR variant in which all cysteines had been removed by mutagenesis (as described in Ref. 17) and which includes a mutation in the first NBD (V510A) to increase protein expression in the cell membrane (18). In this background ("cys-less CFTR") we have mutated individually 22 consecutive amino acids in TM6, from Arg-334 on the outside to Pro-355 on the inside. Use of cys-less CFTR is necessary for these studies because wild-type CFTR is potently inhibited by cytoplasmic methanethiosulfonate (MTS) reagents (11). However, differences in channel function have previously been reported, with cys-less CFTR showing a significantly greater single channel conductance than wild type (17, 18). Mutagenesis was carried-out using the QuikChange site-directed mutagenesis system (Stratagene, La Jolla, CA) and verified by DNA sequencing. All constructs were in the pIRES2-EGFP vector (18) allowing co-expression of cys-less CFTR with enhanced green fluorescent protein. Baby hamster kidney cells were transiently transfected with different cys-less CFTR mutants in this vector as described previously (19), except that 24 h after transfection cells were transferred to 27 °C to promote mature protein expression (18). Cells were used for electrophysiological experimentation after 1–3 days at 27 °C. Individual cells were selected for patch clamp investigation based on identification of enhanced green fluorescent protein expression by fluorescence microscopy.

Macroscopic CFTR currents were recorded using patch clamp recording from inside-out membrane patches excised from baby hamster kidney cells as described in detail previously (20, 21). After patch excision, any pretreatment of the inside-out patch if necessary (see below), and recording of background currents, CFTR channels were maximally activated by exposure to PKA catalytic subunit (20 nM) plus MgATP (1 mM) in the cytoplasmic solution followed by the addition of 2 mM sodium pyrophosphate (PP_i). Both intracellular (bath) and extracellular (pipette) solutions contained 150 mM NaCl, 2 mM $MgCl_2$, and 10 mm TES (pH adjusted to 7.4 using NaOH). Channels were exposed to intracellular and extracellular cysteine-reactive reagents to covalently modify an introduced cysteine. Two MTS reagents, the positively charged [2-(trimethylammonium)ethyl] MTS (MTSET) and the negatively charged [2-sulfonatoethyl] MTS (MTSES), were used. These reagents were initially prepared as high concentration (160 mM) stock solutions in distilled water and stored frozen as small volume aliquots until the time of use, when they were diluted in bath solution and used immediately. MTSES and MTSET were used at high concentrations that were without effect on cys-less CFTR currents (13, 18). Potassium dicyanoaurate ($KAu(CN)_2$) was prepared as a high concentration (100 mM) stock in normal bath solution and added directly to the bath.

Initially high concentrations of MTS reagents (200 μM MTSES or 2 mM MTSET) were applied to the cytoplasmic face of inside-out membrane patches after maximal channel activation, and currents were monitored for at least 5 min until the current had again reached a steady amplitude (see Fig. 1, *A* and *B*). To measure the rate of modification of open channels (see Fig. 5*A*), macroscopic current amplitude was monitored continuously, and the time-dependent change in amplitude after the addition of MTSES was fitted by a single exponential function. In some cases where the rate of modification was very fast the concentration of MTSES was reduced to 20 μM. The time constant of exponential current decay, τ, was used to calculate the apparent second order reaction rate constant, k, from the equation $k = 1/([\text{MTSES}]\tau)$.

In some cases MTS reagents (see Figs. 4–6) and $Au(CN)_2^-$ (see Fig. 7) were used to pretreat inside-out membrane patches (internal application) or intact cells (external application) before recordings. A number of different pretreatment protocols were used. In Fig. 4, channels were pretreated with internal MTSES. After patch excision to the inside-out configuration, 200 μM MTSES was added to the cytoplasmic (bath) solution. MTSES was applied alone (see Fig. 4*C*) or together with PKA (20 nM) and ATP (1 mM) (see Fig. 4*B*). After a 2-min treatment period, all substances were washed from the bath using normal bath solution. After recording of background currents, CFTR channels were then activated using PKA (20 nM), ATP (1 mM), and PP_i (2 mM) as described above and then exposed to a test treatment of MTSES. The same protocol was followed to obtain the data in Fig. 5*B*, except that the duration of pretreatment with MTSES alone was varied (between 10–300 s), and in some cases excised patches were incubated with a lower concentration of MTSES (20 μM) (as indicated on the figure, Fig. 5*B*). Mean data in Fig. 5*B* have been fitted by a single exponential function to determine the modification rate constant for non-activated channels as described above for open channels.

In Fig. 6 channels were pretreated with external MTSET. Intact cells were preincubated in 5 mM MTSET (in normal bath solution) for 5 min following which cells were washed thoroughly with bath solution and transferred to the recording chamber for patch clamp analysis. In Fig. 7, channels were pretreated with internal $Au(CN)_2^-$. The protocol used here was very similar to that for pretreatment with internal MTSES (Fig. 4, see above). After patch excision, 1 mM $KAu(CN)_2$ was added to the bath solution either alone (see Fig. 7*B*) or together with PKA and ATP (see Fig. 7*A*). After a 2-min treatment period, all substances were washed from the bath using normal bath solution, background currents were recorded, and CFTR channels were activated using PKA (20 nM), ATP (1 mM), and PP_i (2 mM) as described above. The same protocol was followed to obtain the data in Fig. 8, except that the duration of pretreatment with $Au(CN)_2^-$ was varied (between 10–300 s) and two different concentrations of $Au(CN)_2^-$ were used (as indicated on Fig. 8, *A* and *B*).

Current traces were filtered at 100 Hz using an 8-pole Bessel filter, digitized at 250 Hz, and analyzed using pCLAMP-10 software (Molecular Devices, Sunnyvale, CA). Macroscopic current-voltage (*I-V*) relationships were constructed using depolarizing ramp protocols (22). Background (leak) currents recorded before the addition of PKA and ATP have been subtracted digitally, leaving uncontaminated CFTR currents (22, 23). As in previous studies (11–13), the shape (rectification) of the *I-V* relationship was quantified as the rectification ratio, and the slope conductance at −80 mV was quantified as a fraction of that at +80 mV. Thus, a rectification ratio of 1 represents a perfectly linear *I-V* relationship, <1 an outwardly rectified *I-V* relationship, and >1 an inwardly rectified *I-V* relationship.

The location of individual amino acid side chains within a recent homology model of CFTR channel structure (24) was

visualized as described recently (13). Briefly, atomic coordinates were obtained from Ref. 24 and visualized using DeepView/Swiss-PdbViewer software. Only TM6, encompassing amino acids Ile-328 (on the outside) to Tyr-362 (on the inside) is illustrated (see Fig. 9). Identified TM6 amino acid side chains only are shown as space-filling atomic models.

Experiments were carried out at room temperature, 21–24 °C. Values are presented as the mean ± S.E. Unless stated otherwise, tests of significance were carried out using an unpaired *t* test, with $p < 0.05$ considered statistically significant. All chemicals were from Sigma, except for PKA (Promega, Madison, WI) and MTSES and MTSET (Toronto Research Chemicals, North York, ON, Canada).

RESULTS

Effect of MTS Modification after Channel Activation—The use of MTS reagents to identify water-exposed cysteine side chains introduced into the CFTR pore region that are accessible from the extracellular solution was first reported in 1994 (25) and have been used by several different groups since that time (26–30). However, intracellular application of these reagents to modify pore cysteines was introduced only recently (11, 13) and has not been used systematically to screen any TM helix. We used site-directed mutagenesis to substitute cysteines for different residues in TM6 in a V510A-cys-less background (see "Experimental Procedures"). Expression of each of these mutants in baby hamster kidney cells led to the appearance of macroscopic PKA- and ATP-dependent currents in inside-out membrane patches (*e.g.* Figs. 1 and 3 and supplemental Fig. S1).

Application of negatively charged MTSES (200 μM) or positively charged MTSET (2 mM) to the intracellular solution after channel activation with PKA, ATP, and PP_i had no significant effect on macroscopic current amplitude in cys-less CFTR (Fig. 1, *A–D*), as reported previously (13), although higher concentrations of MTSES do cause a reversible, voltage-dependent inhibition under these conditions (18). A similar lack of effect was also observed in cys-less R334C, K335C, I336C, T339C, I340C, F342C, S343C, L346C, R347C, V350C, T351C, F354C, and P355C (supplemental Fig. S1 and Fig. 2). However, in nine mutants currents were found to be significantly and rapidly sensitive to application of MTS reagents (Figs. 1, *A* and *B*, and 2 and supplemental Fig. S1). Overall the functional effects of these two MTS reagents on these nine mutants fell into two distinct patterns. Cysteines introduced relatively far along the axis of TM6 from its cytoplasmic end (F337C, T338C, S341C) led to currents that were reduced in amplitude by both MTSES and MTSET application (Figs. 1, *A–D*, and 2). In contrast, substitution of cysteines closer to the cytoplasmic end of TM6 (I344C, V345C, M348C, A349C, R352C, Q353C) gave currents that were increased in amplitude after MTSET application and (with the exception of R352C) decreased in amplitude after MTSES application (Figs. 1, *A–D*, and 2 and supplemental Fig. S1). These effects of MTS reagents were not reversed by washing the reagents from the bath (see also Fig. 4*C*); however, even when the MTS reagents were not removed, their effects could be reversed by the addition of 2–5 mM dithiothreitol (DTT) (*e.g.* Fig. 1*E*).

Fig. 2 indicates that in most cases the functional effects of modification by either MTSES or MTSET were the same when measured at hyperpolarized (−80 mV) or depolarized (+80 mV) voltages, suggesting that modification did not significantly alter the shape of the macroscopic *I-V* relationship. Thus, although the decrease in current amplitude after MTSET treatment of T338C was significantly greater when measured at −80 mV compared with +80 mV (Fig. 2) and the MTSET-dependent increase in amplitude in R352C was also significantly greater when measured at −80 mV compared with +80 mV (Fig. 2), in all other cases there was no significant difference in mean MTS effects measured at these two extremes of the voltage range studied (Fig. 2). Effects of MTS modification on the shape of the macroscopic *I-V* relationship were quantified as in previous studies (*e.g.* Refs. 12, 26, and 29). As shown in Fig. 3*A*, several of the cysteine substitutions themselves (R334C, K335C, I336C, T338C, S341C, F342C, R347C, T351C, R352C, Q353C, F354C) led to significant changes in *I-V* relationship shape as quantified by the rectification ratio (see "Experimental Procedures"), suggesting that mutagenesis of these residues has some impact on pore function. However, in most cases *I-V* relationship shape was not significantly affected after application of either MTSES or MTSET (Fig. 3*B*), with MTSES significantly altering *I-V* relationship shape in S341C, I344C, V345C, and M348C only and MTSET altering shape in F337C, T338C, and R352C only. In previous studies it was found that modification by external MTS reagents had strongly charge-dependent effects on *I-V* shape (12, 26, 29), which have been interpreted as reflecting predominantly electrostatic effects of modification on entry of extracellular Cl^- ions into the pore (12, 26). In contrast, the present results suggest there is no clear pattern of charge-dependent effects of modification by internal MTS reagents on *I-V* relationship shape (Fig. 3*C*), perhaps indicating that MTS modification here has significant non-electrostatic effects.

Pattern of MTS Modification before Channel Activation—In Fig. 1 MTS reagents were applied to the cytoplasmic face of membrane patches after maximal CFTR channel stimulation with PKA, ATP, and PP_i. For this reason we assume that functional modification predominantly reflects MTS reagent reaction with open CFTR channels, although it is conceivable that modification occurs during infrequent interburst channel closures under these conditions. We were interested to know if these same introduced cysteine side chains were also accessible to MTS reagents applied before channel activation. To test this we pretreated inside-out patches with MTSES immediately after excision from the cell but in the absence of PKA or ATP. Under these conditions the channels are closed, and no background current is observed. We investigated five mutants in the central part of TM6 that had readily accessible side chains and that gave robust changes in current amplitude in response to MTSES and MTSET: T338C, S341C, I344C, V345C, and M348C (see Fig. 2).

Fig. 4*A* shows the extent of inhibition of macroscopic current in each of these mutants that results from application of cytoplasmic MTSES (200 μM) after channel activation with PKA, ATP, and PP_i. In each case the inhibition was very rapid after the addition of MTSES to the bath, and modification appeared

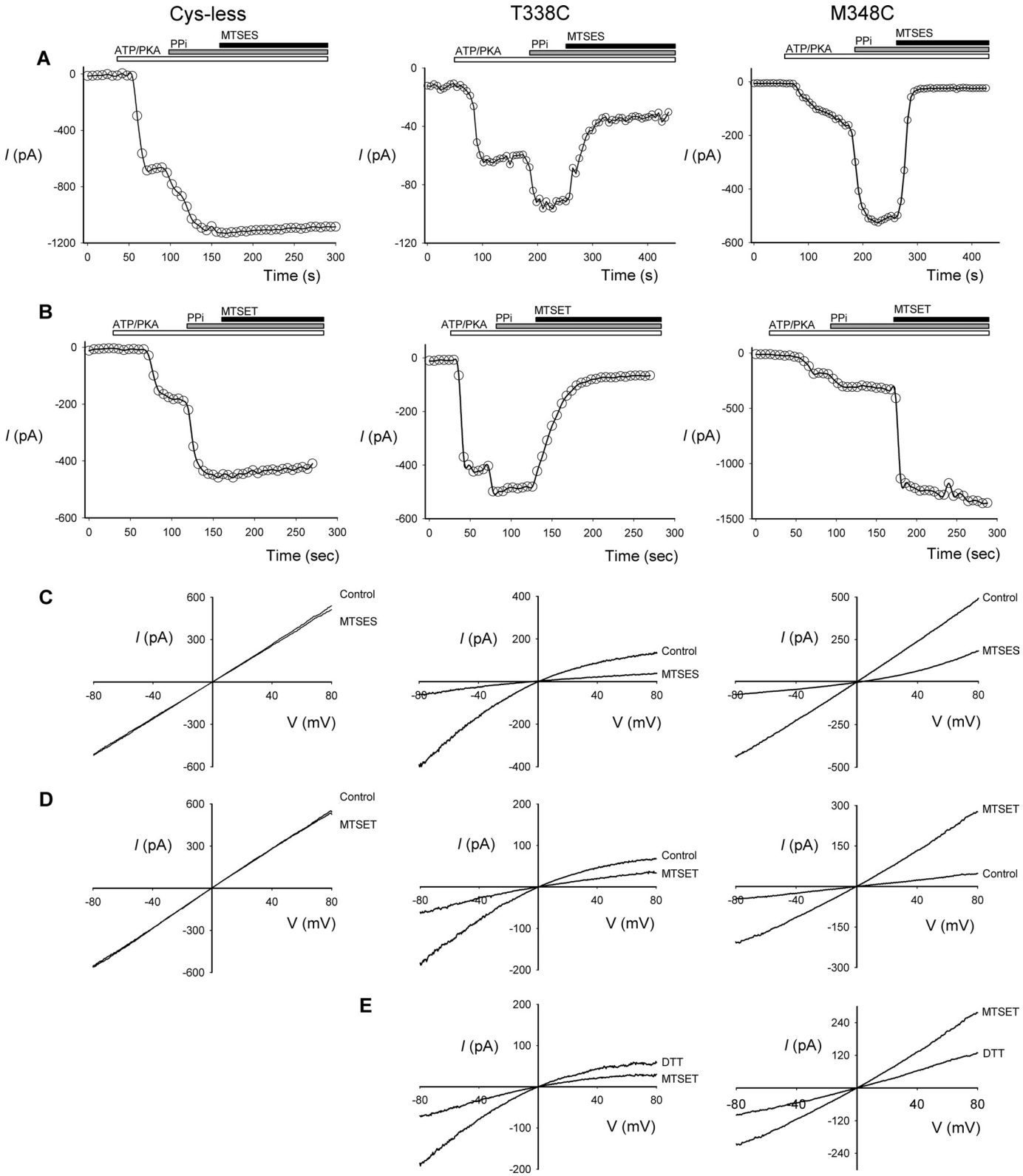

FIGURE 1. **Modification of cysteine-substituted CFTR-TM6 mutants by internal MTS reagents.** *A* and *B*, shown are example time-courses of macroscopic currents (measured at −50 mV) carried by cys-less CFTR, T338C, and M348C in inside-out membrane patches. After patch excision and recording of baseline currents, patches were treated sequentially with PKA (20 nM) and ATP (1 mM), PP_i (2 mM), and either MTSES (200 μM) or MTSET (2 mM). Note that whereas these MTS reagents have no effect on cys-less CFTR current amplitude, they cause rapid inhibition or augmentation of current carried by these two mutants. *C–E*, shown are example leak subtracted *I-V* relationships for these same three channel variants recorded from inside-out membrane patches after maximal channel activation with PKA (20 nM), ATP (1 mM), and PP_i (2 mM). *C* and *D*, currents were recorded before (*Control*) and after application of MTSES (200 μM, *C*), or MTSET (2 mM, *D*) to the intracellular (bath) solution. *E*, shown is the effect of DTT (5 mM) applied after MTSET treatment in T338C and M348C.

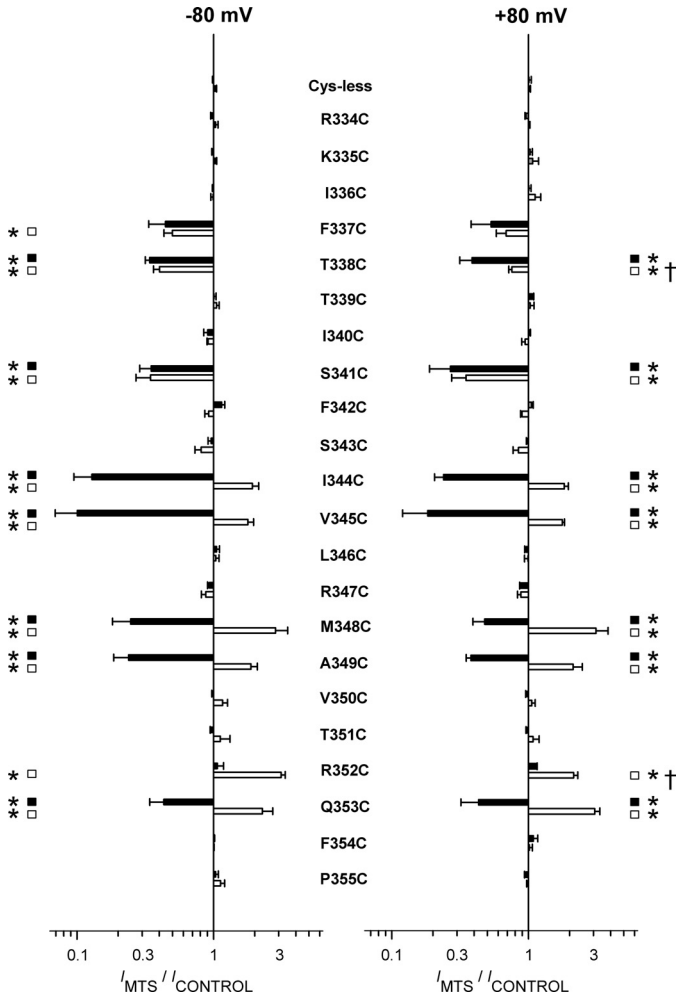

FIGURE 2. **Effects of internal MTS reagents on cysteine-substituted CFTR-TM6 mutants.** Mean effect of treatment with 200 μM MTSES (*black bars*) or 2 mM MTSET (*white bars*) on macroscopic current amplitude in cys-less CFTR and in each of 22 different cysteine substituted TM6 mutants. Effects of these two MTS reagents were quantified by measuring current amplitudes at membrane potentials of −80 mV (*left*) and +80 mV (*right*) before and after complete modification had taken place. Data are the means from 3–5 patches. *Asterisks* indicate a significant difference from cys-less, and *daggers* indicate a significant difference from the same treatment at −80 mV ($p < 0.05$ in both cases).

complete in less than 2 min (see Fig. 5*A*). Fig. 4, *B* and *C*, show the effects of MTSES application under similar conditions, again following maximal channel stimulation with PKA, ATP, and PP_i, but in these cases in inside-out patches that had been pretreated with intracellular MTSES (200 μM for a two-min pretreatment interval) under two different sets of conditions (see "Experimental Procedures"). In Fig. 4*B*, patches were pretreated with MTSES in the presence of PKA and ATP after patch excision, whereas in Fig. 4*C* inside-out patches were pretreated with MTSES alone. In this way, we expect MTSES to have access to both open and closed channels in Fig. 4*B* but only to closed channels in Fig. 4*C*. In both cases, after the 2-in pretreatment period, all drugs were thoroughly washed from the bath, and channels were activated by PKA, ATP, and PP_i before re-exposure to MTSES. For each mutant, in patches that had been pretreated with MTSES, PKA, and ATP and then washed, only small currents were activated by subsequent exposure to PKA, ATP, and PP_i. Furthermore, these small currents were not affected by subsequent re-exposure to MTSES (Fig. 4*B*). This finding confirms that these cysteine side chains were covalently modified by MTSES during pretreatment and that these effects of MTSES were not simply reversed by washing MTSES from the bath. However, different results were obtained when patches were pretreated with MTSES in the absence of stimulants (Fig. 4*C*). Both V345C and M348C again gave only small currents after stimulation with PKA, ATP, and PP_i, and these currents appeared refractory to the re-addition of MTSES, suggesting they had again been irreversibly modified during the pretreatment period. In striking contrast, T338C, S341C, and I344C gave robust currents in response to PKA, ATP, and PP_i, and these currents were strongly inhibited by re-exposure to MTSES (Fig. 4*C*). This result suggests that cysteine side chains introduced at these three positions are modified by MTSES very slowly, if at all, in channels that have not been activated. These findings are summarized in Fig. 4*D*, which illustrate the mean effects of MTSES under the three sets of conditions shown in Fig. 4, *A*–*C*.

To obtain quantitative information on the apparent state dependence of MTSES modification, we compared the apparent rate of modification in activated *versus* non-activated channels. Modification rate in activated channels was estimated from the time course of macroscopic current inhibition caused by application of MTSES after channel activation with PKA, ATP, and PP_i (Fig. 5*A*). Modification was very rapid at I344C, V345C, and M348C under these conditions, such that a lower concentration of MTSES (20 μM) was used to give a measurable rate of current decay (Fig. 5*A*). Modification was considerably slower in T338C and S341C (Fig. 5*C*), suggesting that even in open channels there is some factor restricting MTSES access to these sites. The time-course of modification in non-activated channels was monitored using a protocol similar to that used in Fig. 4*C*. After patch excision, inside-out patches were pretreated with MTSES (20 or 200 μM) for different periods of time (10–300 s) after which all drugs were thoroughly washed from the bath and channels activated by PKA, ATP, and PP_i. Channels were then exposed to a test dose of MTSES (200 μM) to evaluate the extent of MTSES modification that had occurred during the pretreatment period (supplemental Fig. S2). As shown in Fig. 5*B*, both V345C and M348C were apparently rapidly modified by pretreatment with only 20 μM MTSES, as determined by a loss of sensitivity to MTSES upon re-exposure after channel activation. Exponential fitting of the time-course of loss of MTSES sensitivity (Fig. 5*B*) suggested that the modification rate constant was only slightly reduced compared with open channels (Fig. 5*C*), by ~7-fold in V345C and ~4-fold in M348C. In contrast, I344C, S341C, and T338C did not appear to be modified by pretreatment with 200 μM MTSES, even when the pretreatment period was extended to 5 min. After this prolonged pretreatment period, the inhibition of current carried by these three mutants caused by the test dose of MTSES was not significantly different from patches in which no pretreatment had taken place (supplemental Fig. S2; Fig. 5*B*). It is possible that this protocol might not be able to detect small changes in MTSES sensitivity caused by modification of a small fraction of channels during pretreatment. However, even conservatively assuming that 25% of channels could be modified

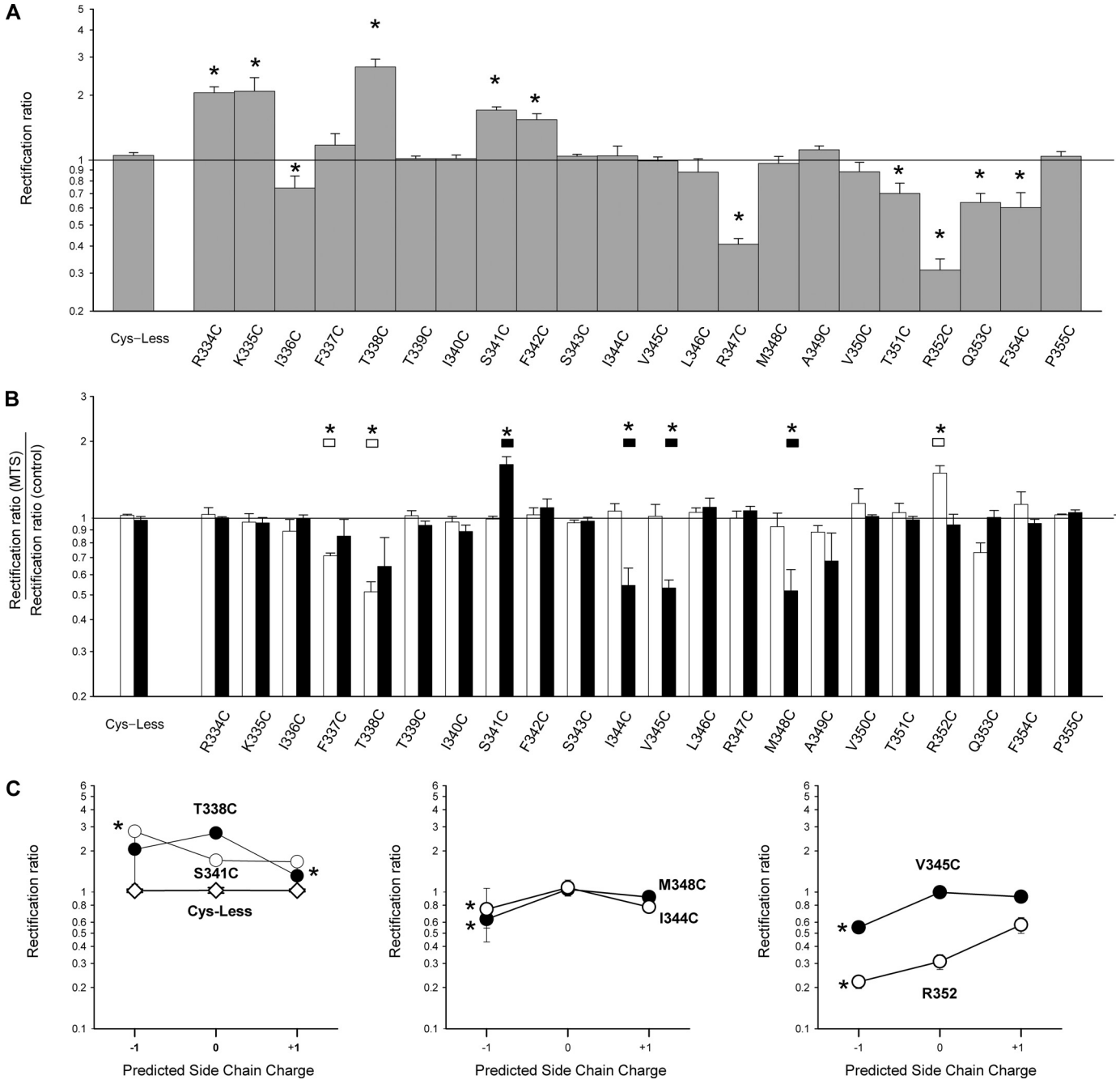

FIGURE 3. **Effect of MTS reagents on *I-V* relationship shape.** *A*, shown is the mean rectification ratio (calculated as described under "Experimental Procedures") for cys-less and each of the mutants used in the present study measured under control conditions for currents activated by PKA (20 nM), ATP (1 mM), and PP_i (2 mM). *Asterisks* indicate a significant difference from cys-less ($p < 0.05$). *B*, shown is the effect of internal MTSET (*white bars*) or MTSES (*black bars*) on the rectification ratio in each channel variant. *Asterisks* indicate a significant difference from cys-less ($p < 0.05$). *C*, shown are mean rectification ratios for selected channel variants under control conditions and after modification with charged MTS reagents, plotted as a function of predicted side chain (−1 with MTSES, 0 control, and +1 with MTSET). *Asterisks* indicate a significant difference from the corresponding rectification ratio under control conditions ($p < 0.05$). Data are the means from 3–8 patches. Where no *error bars* are visible, these are smaller than the size of the symbol.

during a 5-min pretreatment (leading to a 25% decrease in MTSES sensitivity upon re-exposure), we estimate this would reflect a channel modification rate constant of $<5\ M^{-1}\ s^{-1}$ during the pretreatment period. We, therefore, consider that the rate of MTSES modification of T338C, S341C, and I344C before channel activation to be somewhere between 0 and 5 $M^{-1}\ s^{-1}$, or at least 26-fold (for T338C and S341C) to >450-fold (for I344C) less than the estimated rate of modification of activated channels (Fig. 5*C*).

Pattern of Modification by External MTSET—MTS reagents are not thought to be permeant in CFTR (28, 30), an idea that is apparently confirmed by the present study (see "Discussion"). However, the depth to which MTS reagents can penetrate into the CFTR pore when present in the extracellular solution is not clear, with conflicting reports existing as to which TM6 residues can be modified by external MTS reagents (28–31). Most importantly, cysteines introduced in the central region of TM6, including at Thr-338, Ser-341, and Ile-344, have been found to

be accessible to external MTS reagents in some studies but inaccessible in others (summarized in Ref. 30). We used the susceptibility of these and other cysteines introduced into TM6 to internal MTSES (see above) as a novel way to probe the accessibility of these residues to external MTSET. We used MTSET in these experiments as we have previously found it to be a less state-dependent probe of the outer pore than MTSES (29). In these experiments intact cells were exposed to a high concentration of MTSET (5 mM) for 5 min. Cells were then washed and transferred to the experimental chamber for patch clamp analysis. After patch excision to the inside-out configuration, CFTR channels were activated using PKA, ATP, and PP_i and subsequently treated with intracellular MTSES (200 μM) as in Figs. 1 and 4. As shown in Fig. 6*B*, patches excised from cells expressing either T338C or S341C gave only small, outwardly rectified currents under these conditions, and these currents were insensitive to internally applied MTSES. In contrast, I344C, V345C, and M348C gave large currents that showed similar strong sensitivity to internal MTSES as those seen in patches excised from cells that had not been pretreated with MTSET (Fig. 6, *A* and *B*). These findings, summarized in Fig. 6*C*, imply that although T338C and S341C had been modified irreversibly by extracellular MTSET during the pretreatment period, rendering them refractory to inhibition by intracellular MTSES, cysteines substituted for residues located further along the axis of TM6 from the outside (Ile-344, Val-345, Met-348) were not modified by pretreatment with extracellular MTSET. The finding that cysteines introduced close to the cytoplasmic end of TM6 were not modified by external MTSET is important because it suggests that MTSET is not able to enter into cells during the pretreatment period and modify channels from their cytoplasmic end. The change in *I-V* relationship shape seen in T338C and

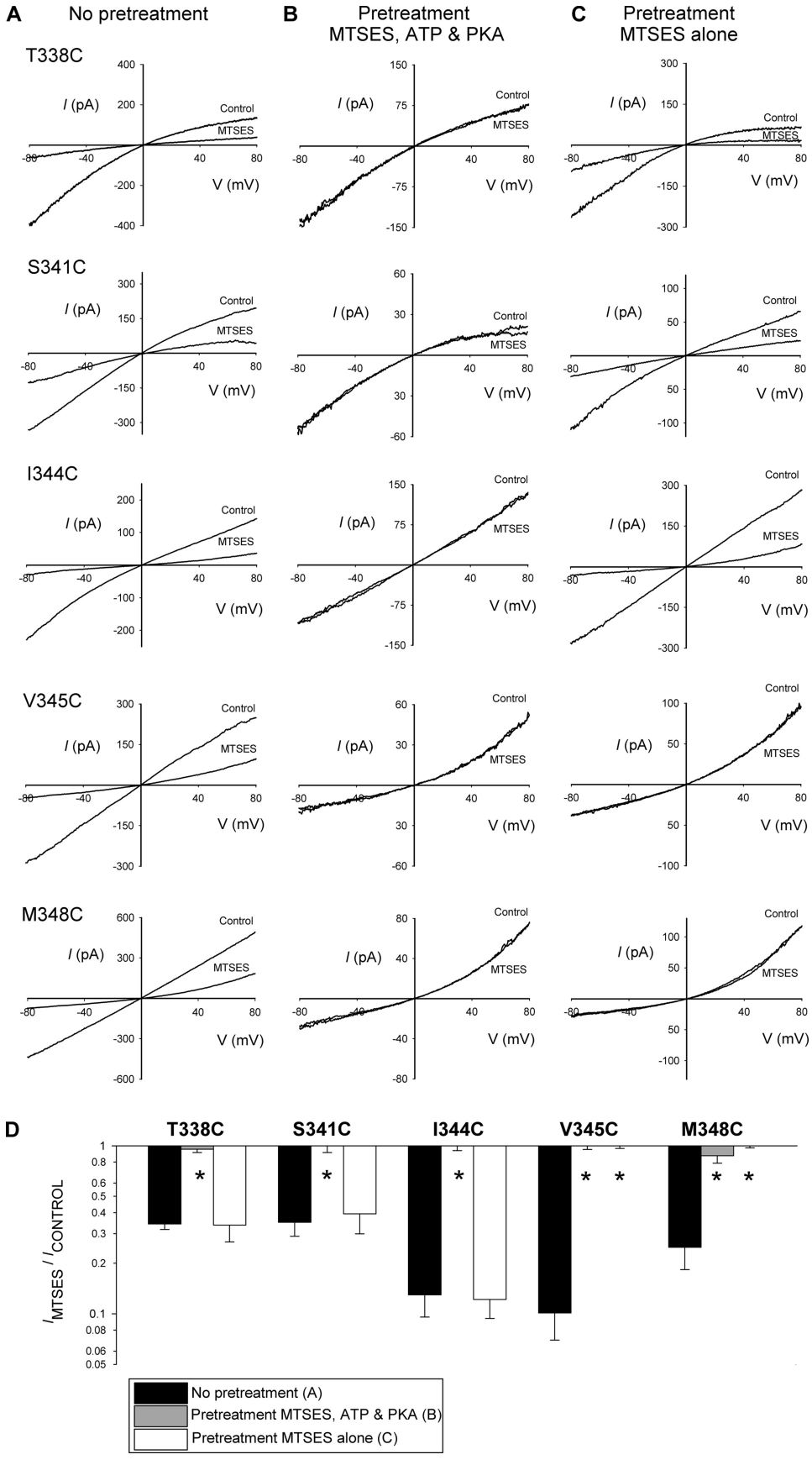

S341C after pretreatment with extracellular MTSET (Fig. 6*D*) is consistent with that reported previously (29) for these mutants in a wild-type (as opposed to cys-less) channel background, a finding used in that study as evidence that modification of the introduced cysteine had taken place. In contrast, the shape of the *I-V* relationship was not significantly changed by MTSET pretreatment in I344C, V345C, or M348C (Fig. 6*D*).

State-dependent Modification by Intracellular Au(CN)$_2^-$—The results shown in Fig. 5 suggest that the accessibility of MTSES from the intracellular solution to the pore is different in activated *versus* non-activated channels. To investigate if permeant anions show the same regulated access to the pore, we used Au(CN)$_2^-$, a highly permeant anion that has been used previously to covalently modify cysteine side chains introduced throughout TM6 (30, 32). As described above for MTSES (Fig. 4), we pretreated inside-out patches with a high concentration of intracellular Au(CN)$_2^-$ (1 mM, for 2 min) after patch excision from cells either with or without co-treatment with PKA and ATP to activate CFTR channels. Again as for MTSES pretreatment (Fig. 4), Au(CN)$_2^-$ and stimulants were then washed thoroughly from the bath, channels were maximally activated with PKA, ATP, and PP$_i$, and sensitivity to intracellular MTSES was quantified. As shown in Fig. 7, Au(CN)$_2^-$ pretreatment did not prevent the inhibitory effects of intracellular MTSES on S341C, I344C, V345C, or M348C irrespective of whether the Au(CN)$_2^-$ was applied to activated or non-activated channels. The most likely explanation of these results is that Au(CN)$_2^-$ failed to modify irreversibly the cysteine side chains at these positions. In contrast, Au(CN)$_2^-$ pretreatment did prevent the inhibitory effects of MTSES on T338C but only if applied together with PKA and ATP. Thus, after pretreatment with Au(CN)$_2^-$ together with PKA and ATP, T338C gave only small currents that were not significantly affected by the addition of MTSES (Fig. 7, *A* and *C*), whereas after pretreatment with Au(CN)$_2^-$ alone, T338C gave large currents with strong sensitivity to MTSES (Fig. 7, *B* and *C*). This suggests that T338C, in contrast to the other mutants studied in Fig. 7, was covalently modified by Au(CN)$_2^-$ pretreatment but only if applied to activated channels. Thus, access of permeant Au(CN)$_2^-$ ions to this part of the pore, as with MTSES, is greatly impaired before channel activation.

Because Au(CN)$_2^-$ can act as an open channel blocker in CFTR (21), the time-course of covalent modification of T338C by Au(CN)$_2^-$ was quantified using a pretreatment protocol such as those used in Figs. 5*B* and 7. After patch excision, inside-out patches were pretreated with Au(CN)$_2^-$ alone (1 mM) or Au(CN)$_2^-$ (2 μM) together with PKA and ATP for different periods of time. All drugs were then thoroughly washed from the bath and channels activated by PKA, ATP, and PP$_i$. Channels were then exposed to MTSES (200 μM) to evaluate the degree of Au(CN)$_2^-$ modification that had occurred during the pretreatment period (supplemental Fig. S3). As shown in Fig. 8, there was no evidence that non-activated T338C channels were modified by even 1 mM Au(CN)$_2^-$ pretreatment; after 5 min of pretreatment, the sensitivity of current to inhibition by MTSES was not significantly reduced ($p > 0.5$) (Fig. 8*A*). Using the same logic applied above to modification by MTSES, we conservatively estimate a channel modification rate by Au(CN)$_2^-$ of <1 M^{-1} s^{-1} during the pretreatment period. In contrast, T338C channels appeared readily modified by a much lower dose of Au(CN)$_2^-$ when applied to activated channels in the presence of PKA and ATP (Fig. 8*B*); exponential fitting of the time-course of loss of MTSES sensitivity suggests an Au(CN)$_2^-$ modification rate constant of 20,500 M^{-1} s^{-1} under these conditions.

DISCUSSION

Structure of TM6 and Location within the Permeation Pathway—It has long been known that TM6 plays a key role in forming the CFTR pore and determining its functional properties (9, 10). The functional importance of TM6 to the pore is also implied by atomic homology models of the whole CFTR protein (24, 33, 34). Indeed, the location of solvent-exposed amino acid side chains in TM6 that presumably line the pore has been investigated using substituted cysteine accessibility mutagenesis and modification by external MTS reagents by several different groups (28–31), with somewhat disparate results (summarized in Ref. 30). Our results show for the first time that cysteines substituted for nine different residues in TM6, Phe-337, Thr-338, Ser-341, Ile-344, Val-345, Met-348, Ala-349, Arg-352, and Gln-353, are covalently modified by intracellular MTSES and MTSET applied after channel activation (Fig. 2 and supplemental Fig. S1). This suggests that the side chains at each of these sites line the pore and are accessible to the intracellular solution in open channels. In contrast, cysteines substituted for residues closer to the outer end of TM6, at Arg-334, Lys-335, and Ile-336, are inaccessible to internal MTS reagents (Fig. 2) even though previously published evidence strongly favors the idea that each of these side chains is accessible to externally applied MTS reagents (26–31). This result suggests that MTS reagents are not significantly permeant in CFTR channels and that some constriction in the pore prevents MTS reagents applied to one side of the membrane from modifying cysteine side chains on the other side of this constriction. The same conclusion was previously reached by Alexander *et al.* (30) using externally applied MTS reagents.

Interestingly, our results indicate directly that cysteines substituted for both Thr-338 and Ser-341 can be modified by both internal *and* external MTS reagents (Figs. 2 and 6). Previously published data concerning the accessibility of each of these two residues to external MTS reagents, investigated using the func-

FIGURE 4. **Modification of introduced cysteines during pretreatment with internal MTSES.** *A–C*, example leak-subtracted *I-V* relationships for five highly MTSES-sensitive mutants (T338C, S341C, I334C, V345C, M348C) showing the effects of application of internal MTSES (200 μM) after maximal channel activation with PKA (20 nM), ATP (1 mM), and PP$_i$ (2 mM). Patches have been pretreated in three different ways (see "Experimental Procedures"), no pretreatment (*A*), pretreated with MTSES (200 μM), PKA, and ATP for 2 min (*B*), and pretreated with MTSES alone (200 μM) for 2 min (*C*). Note that for each mutant, after pretreatment with MTSES, PKA, and ATP, stimulated currents were small and apparently refractory to the effects of internally applied MTSES (*B*), suggesting that channels had been covalently modified during the pretreatment. *D*, shown is the mean effect of internal MTSES on macroscopic current amplitude at −80 mV in each of the three protocols shown in *A–C*. *Asterisks* indicate a significant difference from control (no pretreatment, *A*) conditions ($p < 0.01$). Data are the means from 3–4 patches.

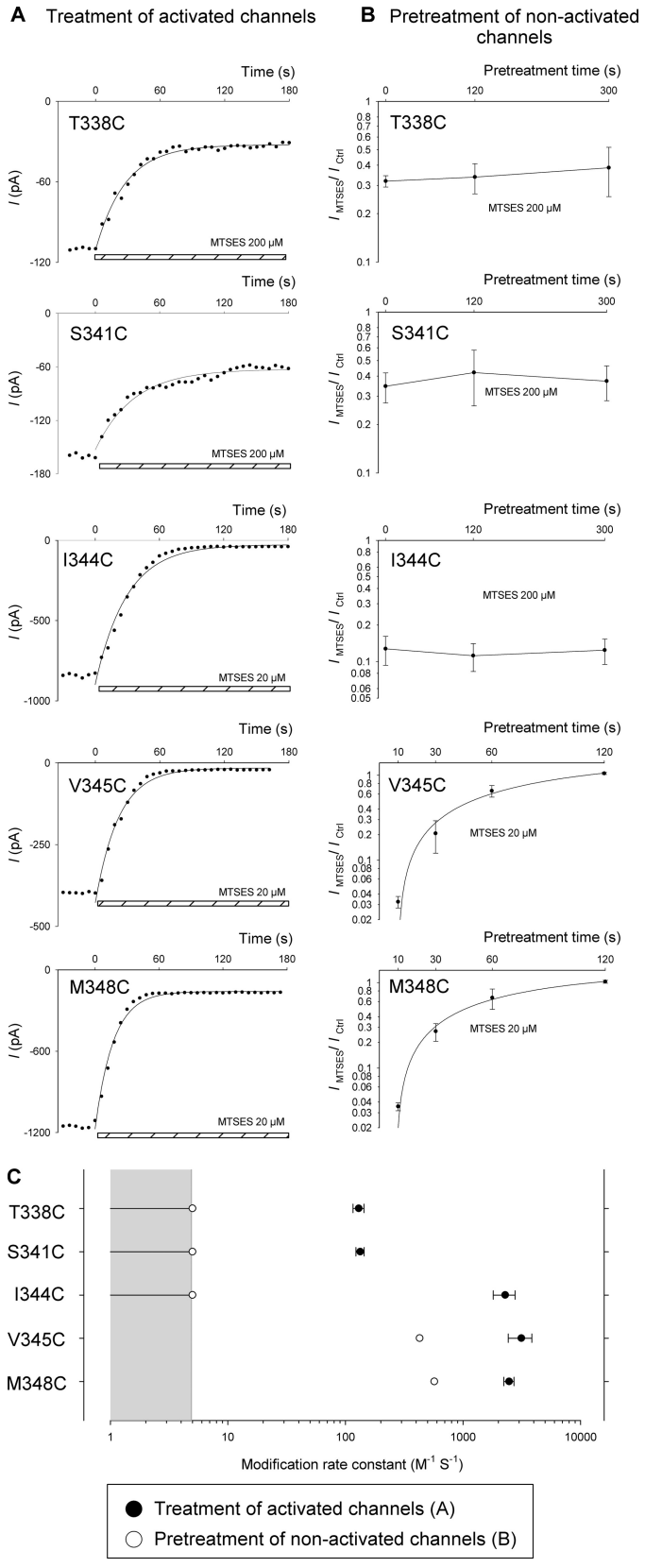

FIGURE 5. **Apparent time-course of modification of activated and non-activated channels by internal MTSES.** *A,* shown are example time-courses of macroscopic currents (measured at −50 mV) carried by the named variants in inside-out membrane patches. Currents amplitudes were measured every 6 s after attainment of stable current amplitude after channel activation with PKA (20 nM), ATP (1 mM), and PP_i (2 mM). In each case MTSES (200 μM for T338C and S341C; 20 μM for I344C, V345C, and M348C) was applied to the cytoplasmic face of the patch at time 0 (as indicated by the *hatched bar* at the *bottom of each panel*). The decline in current amplitude after MTSES application has been fitted by a single exponential function in each case. *B*, shown is the mean effect of internal MTSES (200 μM) on macroscopic current amplitude at −80 mV after maximal channel activation with PKA (20 nM), ATP (1 mM), and PP_i (2 mM). Patches were pretreated with MTSES (200 μM for T338C, S341C, and I344C; 20 μM for V345C and M348C) for variable periods of time indicated on the *abscissa*. Data for V345C and M348C have been fitted by an exponential function to estimate the rate of modification of non-activated channels. For T338C, S341C, and I344C, there was no significant change in apparent MTSES sensitivity even after pretreatment with 200 μM MTSES for 5 min ($p > 0.5$), suggesting that no significant degree of modification had taken place in these channels during the pretreatment period. Data are the means from 3–5 patches at each pretreatment time. *C*, shown are calculated MTSES modification rate constants for open channels (●, *A*) or non-activated channels (○, *B*). Because a modification rate constant could not be calculated for non-activated T338C, S341C, or I344C channels, we conservatively estimate a value between 0 and 5 M^{-1} s^{-1} (*gray area*, see "Results," "Pattern of MTS Modification before Channel Activation"). Data are the means from 3–6 patches for open channels (●).

tional effects of MTS exposure, had yielded conflicting results. Thus, Thr-338 was judged to be accessible from the outside in some studies (28–30, 35) but not others (31), and Ser-341 was also considered accessible by some groups (29, 31) but inaccessible by others (28, 30). We believe that the protocol we have used, which demonstrates that external MTSET prevents the effects of internal MTSES, presumably by covalently modifying the only cysteine side chain in the cys-less T338C or S341C protein, offers an alternative approach to investigating the accessibility of these side chains from the outside. Thus, whereas previous studies relied on changes in macroscopic current amplitude resulting from modification, the protocol we have used is independent of whether or not modification by external MTSET alters current amplitude. On the intracellular side of these residues, at I344C, V345C, and M348C, substituted cysteines were apparently accessible to internal MTS reagents (Figs. 2 and 4) but not to external MTSET (Fig. 6). This finding is consistent with these side chains being exposed within the pore on the intracellular side of a constriction in the pore that prevents the passage of MTS reagents (30).

Our results concerning the accessibility of substituted cysteines in open channels are summarized in Fig. 9*A*. At the extracellular end of TM6 are residues that are accessible to MTS reagents only from the outside, and at the intracellular end are residues that are accessible only from the inside. We speculatively designate these residues as existing within functionally distinct regions of the pore, the "outer vestibule" and "inner vestibule" of the pore, respectively. The distinct sidedness of modification observed in these two putative regions of the pore is again consistent with the inability of MTS reagents to permeate through the pore. In the center of TM6 are residues that are apparently accessible from both sides of the membrane. We suggest that these residues exist within the narrowest region of the pore, where they can be reached by at least the reactive part of MTS reagents applied to either end of the pore, presumably without the entire MTS molecule needing to permeate through the channel. For example, structural flexibility of this narrow region of the pore may allow MTS reagents to access this region at a low rate from either end of the pore. Alternatively, it is possible that the accessibility of these residues switches in different channel conformations, being exposed

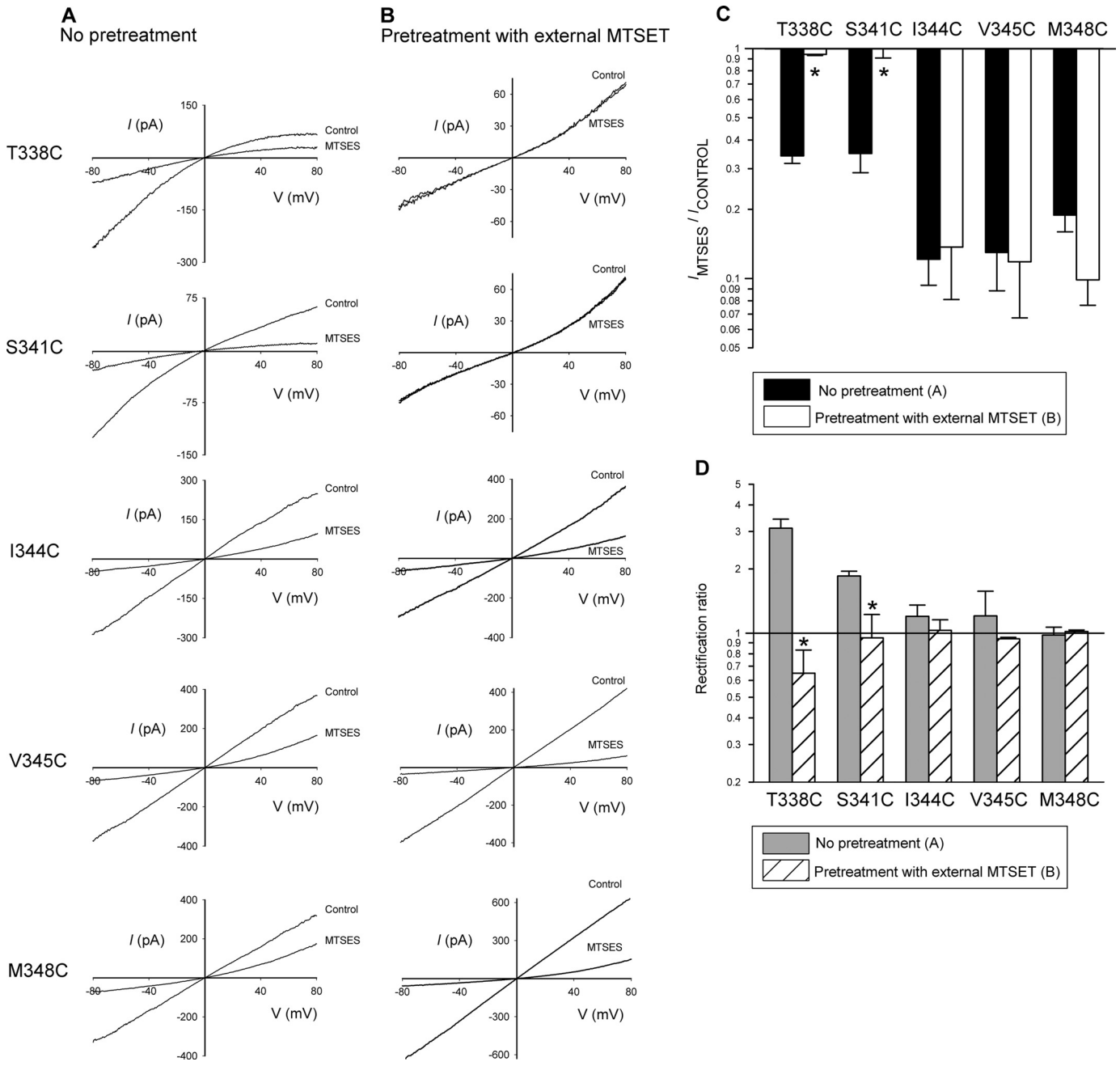

FIGURE 6. **Modification of introduced cysteines by pretreatment with external MTSET.** *A* and *B*, shown are example leak-subtracted *I-V* relationships for each of the five mutants named, showing the effects of application of internal MTSES (200 μM) after maximal channel activation with PKA (20 nM), ATP (1 mM), and PP_i (2 mM). Patches were excised from cells that had been pretreated in two different ways (see "Experimental Procedures"), no pretreatment (*A*), pretreated with external MTSET (5 mM, for 5 min, *B*). *C*, shown is a comparison of the effects of MTSES on macroscopic current amplitude at −80 mV after the two different pretreatments shown in *A* and *B*. The *asterisk* indicates a significant difference from no pretreatment conditions ($p < 0.005$). *D*, shown is the mean rectification ratio for control CFTR currents (recorded before exposure to internal MTSES) under these two sets of conditions, indicating that pretreatment with external MTSET significantly decreases the rectification ratio in both T338C and S341C (*asterisks*, $p < 0.05$). Data are the means from 3–8 patches.

to the outside in one conformation and to the inside in another conformation. Each of these possibilities is consistent with a wealth of functional data based on site-directed mutagenesis studies suggesting that the region around Phe-337, Thr-338, and Ser-341 is the narrowest part of the open CFTR pore (9, 10). Interestingly, quantitative analysis of the rate of MTSES modification in open channels (Fig. 5*C*) suggests that the modification rate constant for residues in the putative inner vestibule (I344C, V345C, M348C) is 17–24-fold larger than for residues in the putative narrow pore region (T338C, S341C), suggesting that even in open channels some obstacle exists restricting (but not preventing) movement of MTSES into the narrow region. We propose that this "obstacle" reflects a physical narrowing of the pore lumen between Ile-344 and Ser-341.

The location of side chains that we designate as being accessible from the outside, the inside, or from both sides, which we suggest correlate approximately with the pore outer vestibule, inner vestibule, and narrow region, within a current atomic homology model of TM6 in the CFTR pore (24) is shown in Fig.

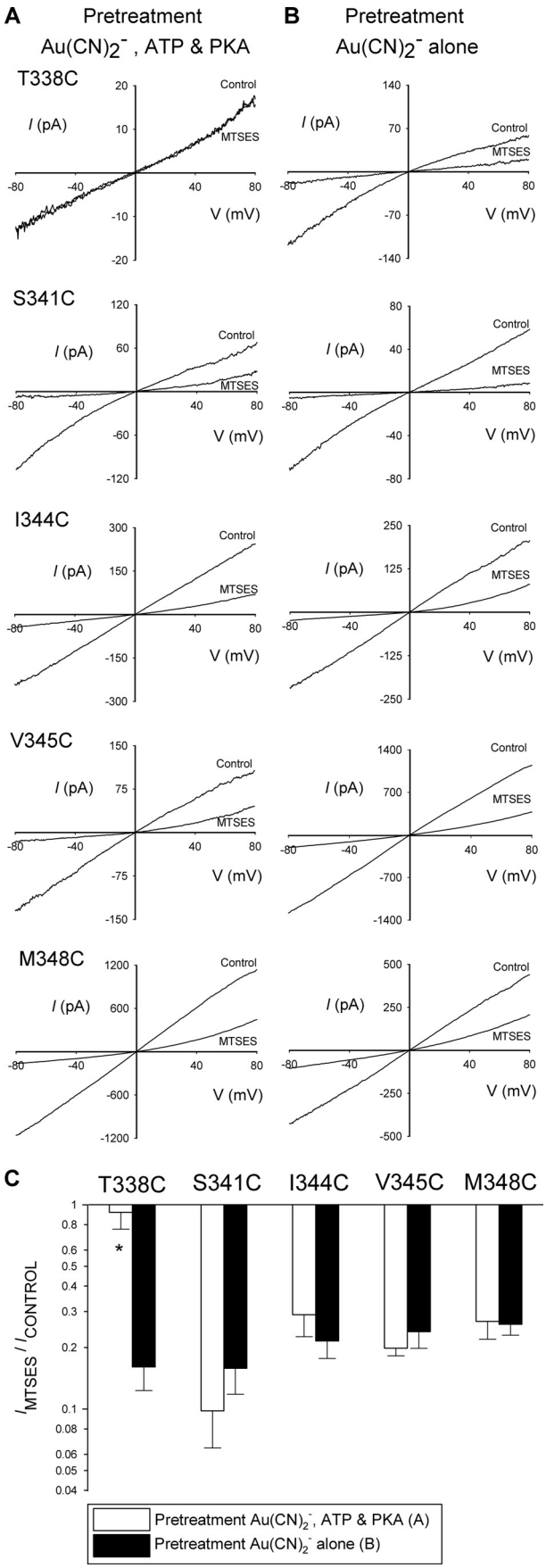

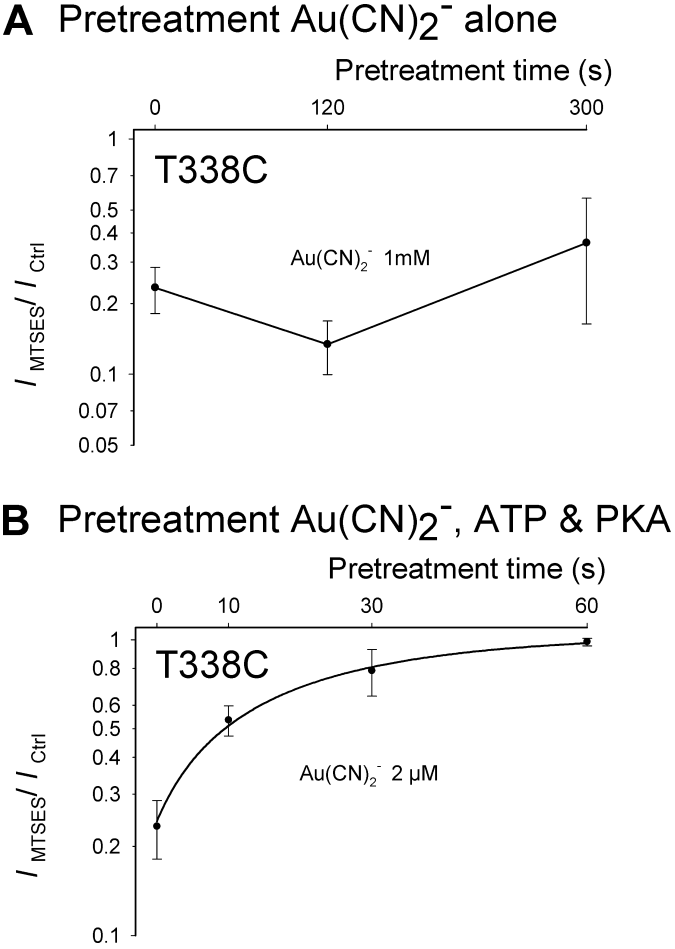

FIGURE 8. **Apparent time-course of modification of activated and non-activated T338C channels by internal $Au(CN)_2^-$.** Mean effect of internal MTSES (200 μM) on macroscopic current amplitude at −80 mV after maximal channel activation with PKA (20 nM), ATP (1 mM), and PP_i (2 mM). Patches were pretreated with $Au(CN)_2^-$ alone (1 mM) (*A*) or $Au(CN)_2^-$ (2 μM) in the presence of PKA (20 nM) and ATP (1 mM) (*B*), for variable periods of time indicated on the *abscissa*. Data for pretreatment with $Au(CN)_2^-$, PKA, and ATP have been fitted by an exponential function to estimate the rate of modification of activated channels. For pretreatment of non-activated channels, there was no significant change in apparent MTSES sensitivity even after pretreatment with 1 mM $Au(CN)_2^-$ for 5 min ($p > 0.5$), suggesting that no significant degree of $Au(CN)_2^-$ modification had taken place in these channels during the pretreatment period. Data are the means from 3–4 patches at each pretreatment time.

9*B*. The accessible side chains appear along one face of TM6, adjacent to the aqueous lumen of the pore.

Two arginine residues near the cytoplasmic end of TM6, Arg-347 and Arg-352, have previously been suggested to interact with negatively charged side chains in other TMs, contributing to overall channel architecture (36–38). Our results showing that R347C is inaccessible to internal MTS reagents

FIGURE 7. **State-dependent modification of T338C by pretreatment with internal $Au(CN)_2^-$.** *A* and *B*, shown are example leak-subtracted *I-V* relationships for each of the five mutants named, showing the effects of application of internal MTSES (200 μM) after maximal channel activation with PKA (20 nM), ATP (1 mM), and PP_i (2 mM). Patches have been pretreated in two different ways (see "Experimental Procedures"), pretreated with $Au(CN)_2^-$ (1 mM), PKA (20 nM) and ATP (1 mM) for 2 min (*A*) and pretreated with $Au(CN)_2^-$ (1 mM) alone for 2 min (*B*). *C*, shown is the mean effect of internal MTSES on macroscopic current amplitude at −80 mV in each of these two $Au(CN)_2^-$ pretreatment protocols. *Asterisks* indicate a significant difference from patches pretreated with $Au(CN)_2^-$ alone ($p < 0.01$). Data are the means from 3–4 patches.

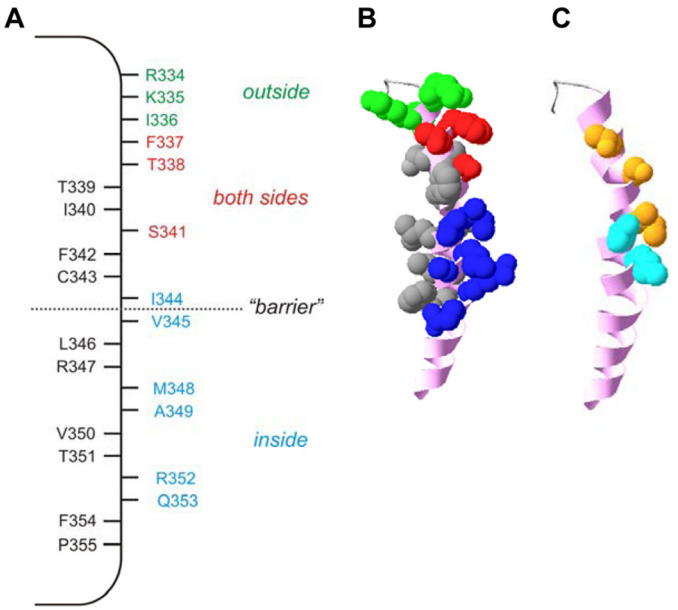

FIGURE 9. **Proposed location of internally exposed side chains in TM6.** *A*, location of residues which, when mutated to cysteine, are exposed to internal MTS reagents only (*blue*), to external MTS reagents only (*green*), or to MTS reagents applied to either side of the membrane (*red*). Other resides that we find not to be modified by internal MTS reagents and presumably not exposed to the pore lumen are shown in *black*. Internal MTS modification is as defined in the present work; external MTS modification as shown in Fig. 6 (T338C, S341C) or in previous work (26, 28–31). Note that F337C has been identified as accessible to external MTS reagents in some previous studies (29, 31) but not in others (28, 30); it is included as pore-lining here because we find it to be accessible to internal MTS reagents (Fig. 2). *B*, shown is the location of these side chains in a recently published atomic homology model of TM6 (24), viewed from the side. Side chains allocated as accessible from the outside, accessible from the inside, accessible from both sides, or inaccessible, are colored as in *A*, whereas the TM6 helical backbone is colored *pink*. *C*, shown is the proposed location of state-dependent change in side chain accessibility in the same model of TM6. Side chains accessible only in activated channels (Thr-338, Ser-341, Ile-344) are colored *orange*, and those accessible both in activated and non-activated channels (Val-345, M348) are in *cyan*. Other side chains are not shown.

(Fig. 2) are, therefore, compatible with previous findings that this residue normally forms a salt bridge with Asp-924 in TM8 (36). However, our finding that the increase in R352C macroscopic current amplitude that results from modification by MTSET is significantly larger when measured at −80 mV compared with +80 mV (Figs. 2 and 3) seems initially in conflict with the suggestion that this arginine normally interacts with Asp-993 in TM9 (37, 38) and is instead more consistent with our previous suggestion that this arginine residue normally forms an accessible surface charge near the inner mouth of the pore (11). However, as pointed out by Alexander *et al.* (30), these two suggestions are not necessarily irreconcilable; they suggested that the role of Arg-352 may be to neutralize the effect of an exposed negative charge contributed by the Asp-993 side chain.

Because of the strong sensitivity of wild-type CFTR to internally applied MTS reagents (11), it was necessary for us to carry out our experiments using cys-less CFTR. Because this CFTR variant has a severe trafficking defect (17, 18, 39, 40), several manipulations were necessary to obtain a high enough density of channel protein in the cell membrane for functional analysis (see "Experimental Procedures"). Nevertheless, once present in the cell membrane, cys-less CFTR appears to function normally (17, 18, 30, 39), and we believe that the structural inferences drawn from our work are applicable to wild-type CFTR. However, it is known that differences in pore function do exist between wild-type and cys-less CFTR; for example, cys-less has a significantly higher single channel conductance (17, 18). It is, therefore, possible that movement of MTS reagents in the pore of these two channel variants may be different, potentially clouding the applicability of our present results to the wild-type CFTR channel pore.

Our results concerning the functional effects of intracellular MTS modification reveal another pattern, namely that modification of exposed cysteine side chains by MTSES always led to a reduction in macroscopic current amplitude, whereas the effects of MTSET appeared dependent on the location of the modified side chain along the axis of the pore (Fig. 2). Thus, internal MTSET modification increased macroscopic current amplitude at sites close to the cytoplasmic end of TM6 (I344C, V345C, M348C, A349C, R352C, Q353C) but decreased macroscopic current amplitude at sites further from the cytoplasmic end (F337C, T338C, S341C) (Fig. 2). The universally inhibitory effects of MTSES likely reflect an inhibition of Cl^- permeation that results from deposition of a large, negatively charged group within the permeation pathway. MTSET modification in a physically restricted region of the pore might result in steric inhibition of Cl^- flux, as suggested previously (13). In contrast, MTSET modification in a wide region of the pore may increase Cl^- flux, for example via enhanced electrostatic attraction of Cl^- ions. Indeed, MTSET modification of cysteines introduced at numerous sites in the CFTR pore outer vestibule has previously been shown to increase single channel Cl^- conductance (12, 26). Our finding that MTSET modification of cysteines in the putative narrow pore region (in F337C, T338C, S341C) reduces macroscopic Cl^- current amplitude, whereas modification of cysteines in the putative pore inner vestibule (I344C, V345C, M348C, A349C, R352C, Q353C) increases macroscopic current amplitude would appear consistent with such a separation of steric *versus* electrostatic effects. However, it would be expected that an increase in electrostatic attraction due to positive charge deposition in the pore inner vestibule would have a greater effect on currents carried by Cl^- efflux compared with those carried by Cl^- influx, leading to strongly voltage-dependent effects of modification on Cl^- current amplitude. Such an apparently electrostatic effect was observed for modification of R303C in TM5 by internal MTS reagents (11) and also for cysteines introduced in the outer parts of TMs 11 and 12 by external MTS reagents (12). In contrast, we find the effects of MTSET modification on current amplitude to be independent of voltage in most cases (Fig. 2), arguing against a purely electrostatic effect. Furthermore, it has recently been shown that adding an additional positive charge in the pore inner vestibule by mutagenesis has only very minor effects on Cl^- unitary conductance (13), whereas we see increases in macroscopic current amplitudes of 1.8–6-fold after MTSET modification (Fig. 2). Single channel recording will be necessary to fully understand the mechanism by which MTSET deposition within the pore increases macroscopic Cl^- current amplitude, assuming that the conductance of the cysteine-substituted mutants is large enough for single channel analysis. Whatever

the reason for this increase in macroscopic current amplitude, it does appear to be a consistent, rather than site-specific, effect of modification of cysteines in the putative pore inner vestibule (Fig. 2).

Previously it has been suggested that external $Au(CN)_2^-$ can covalently modify cysteines introduced at multiple sites throughout TM6 (30). The use of $Au(CN)_2^-$ as a probe added to the intracellular solution is complicated by the fact that this lyotropic anion causes high affinity voltage-dependent block of the pore (21) that is strongly affected by non-cysteine substitutions in TM6 (19, 41). We used a pretreatment protocol to identify cysteines that were covalently (irreversibly) modified by intracellular $Au(CN)_2^-$. To our surprise we found no evidence that S341C, I344C, V345C, or M348C was modified by pretreatment with a high concentration of $Au(CN)_2^-$ (1 mM) irrespective of whether it was applied to active or inactive channels (Fig. 7). This was presumably not a technical problem with our pretreatment protocol as it appears that T338C can be irreversibly modified by pretreatment with $Au(CN)_2^-$ in this way (Fig. 7). Our results suggest that these other cysteine side chains either are not covalently modified by $Au(CN)_2^-$ or that the modification is not irreversible and can relatively easily be reversed by washing. Previously it was suggested that externally applied $Au(CN)_2^-$ could covalently modify cysteine side chains in TM6 including I344C and M348C (30). Why these (and other) cysteine side chains were apparently not irreversibly modified by $Au(CN)_2^-$ in our experiments is not clear and raises questions concerning the use of this substance as a cysteine-reactive reagent.

Regulated Access from the Cytoplasm to the Narrow Pore Region—CFTR is a phosphorylation-dependent, ATP-gated ion channel. It has been proposed that ATP-dependent conformational changes in the NBDs precede and control opening of the channel pore (16, 42, 43), and conformational changes in the pore that are associated with ATP-dependent gating have been identified (28). However, the major changes in pore conformation that are triggered by PKA phosphorylation and ATP binding and hydrolysis and that lead to opening of the permeation pathway are not known. Our present results indicate that access of substances from the intracellular solution to the pore is regulated by the channel activation state. Thus, in phosphorylated, open channels, MTSES can modify residues in the putative inner vestibule (I344C, V345C, M348C) and (albeit more slowly) the putative narrow region of the pore (T338C, S341C) (Figs. 2, 5, and 9*A*). In contrast, before exposure to PKA and ATP, when the channels are presumed to be in a non-activated state, MTSES movement into the pore is much more restricted; whereas V345C and M348C can still be modified (at a slightly reduced rate), the rate of modification in T338C, S341C, and I344C was too small to be quantified (Fig. 5). The modification rate constant for I344C was strikingly different under these two different conditions, being $2289 \pm 480\ M^{-1}\ s^{-1}$ ($n = 3$) in open channels and $<5\ M^{-1}\ s^{-1}$ in non-activated channels. We, therefore. suggest that activation of CFTR involves removal of a barrier in the Cl^- permeation pathway in the region close to TM6 residues Ile-344 and Val-345 (Fig. 9*A*). The location of TM6 side chains that may lie on the inside of this barrier (*i.e.* those that can be readily modified by intracellular MTSES in non-activated channels) and on the outside of this barrier (*i.e.* those for which modification was not apparent in non-activated channels) are indicated on Fig. 9*C*. Importantly, the access of permeant $Au(CN)_2^-$ anions to T338C in the putative narrow region of the pore is also regulated by channel activation, based on the strong PKA and ATP dependence of the apparent rate of modification of T338C by $Au(CN)_2^-$ (Fig. 8).

Based on structural and molecular modeling studies, the CFTR TMDs are thought to exist in different conformational states that may be linked to different phosphorylation and/or nucleotide binding states of the overall protein (34, 44, 45). The different TMD structural conformations observed in CFTR may relate, in some as yet not well understood way, to the "inward facing" and "outward facing" conformational states of other ATP binding cassette proteins that are thought to allow these proteins to act as active transporters by an alternating access model (34, 46, 47). In the alternating access model, it is proposed that the substrate translocation pathway has two gates that are never open at the same time, such that a continuous pathway never exists across the membrane. Indeed, it has been proposed that in the CFTR substrate translocation pathway (channel pore), one gate has atrophied, and only one remains, such that CFTR functions as a "broken pump" in which a continuous pathway (*i.e.* the open channel pore) can exist (34, 48, 49). Based on our present findings, we speculatively suggest that one functionally important structural consequence of the conformational rearrangement in the TMDs is the removal of a functional barrier preventing access from the cytoplasm to residues located in the narrowest region of the pore. The potential relationship between this barrier and dynamic changes in pore conformation that are triggered by ATP binding and hydrolysis in phosphorylated channels remains to be determined.

Although CFTR looks like a pump, it works like a channel, and the presence of a single gate that controls the open-closed transition is a common facet of ion channel function (48). In other channel types, for example, K^+ channels (50–53), nicotinic acetylcholine receptor channels (54), and P2X receptor channels (55), channel opening is controlled by the movement of bulky, hydrophobic side chains out of the permeation pathway, removing a hydrophobic seal that prevents ion passage in the channel closed state. Inspection of Fig. 9*A* indicates that the CFTR channel pore is lined by hydrophobic side chains (Ile-344, Val-345, Met-348) from TM6 around the region that we propose may form a barrier to ion movement in non-activated channels. Although the role of these hydrophobic residues in ATP-dependent channel gating has not yet been investigated directly, it is tempting to speculate that channel opening involves a physical withdrawal of these side chains from the pore, opening a pathway for the movement of Cl^- and other permeant anions. In other channels and transporters other gating mechanisms may exist; for example, in ClC Cl^- channels pore opening may involve withdrawal of a negatively charged amino acid side chain from the Cl^- permeation pathway (56), suggesting that Cl^- movement in closed channels is prevented by an electrostatic, rather than a hydrophobic, barrier.

Apparent state-dependent access to the CFTR pore from the cytoplasm may also have implications for the mechanism of action of open channel blockers. A large number of organic anions have been shown to inhibit CFTR by an open channel block mechanism (57). These substances are thought to bind within the inner vestibule of the pore (10, 58), and although several pore-lining residues have been shown to interact with open channel blockers (13, 58, 59), the physical location of the blocker binding site(s) has not been determined. Our present results suggest that open channel blockers may have access to sites located along the axis of TM6 as far as Val-345 in non-activated channels but may be able to penetrate more deeply into the pore from its cytoplasmic end once channels have been activated. Thus, if blockers interact with a binding site located extracellular to Ile-344 in TM6, our results would predict a state-dependent interaction in which blockers could access their binding site in activated but not in non-activated channels.

Summary—Comparison of our present results investigating the functional effects of modification of cysteines introduced into TM6 by internally applied MTS reagents (Fig. 2) with previous work using externally applied MTS reagents (26, 27) suggests that TM6 contributes to the aqueous lumen of the channel pore along its entire length (Fig. 9*A*). Furthermore, the functional effects of modification by internal and external MTS reagents lead us to propose a model in which the pore is subdivided into functionally distinct "regions" that we refer to as the outer vestibule, narrow region, and inner vestibule (Fig. 9*A*). Before channel activation, access of internally applied MTS reagents to the pore is restricted to residues in the putative inner vestibule, whereas after activation they are able to modify residues apparently located further into the pore, reaching into the narrow region (Figs. 5, 9). Access of permeant $Au(CN)_2^-$ ions from the cytoplasm to the pore narrow region also appears strongly regulated by channel activation state (Figs. 7 and 8). We, therefore, suggest that channel activation involves removal of a restriction, preventing access from the cytoplasm to the narrow region of the pore and tentatively speculate that this mechanism involves removal of a localized barrier to ion movement near the outer end of the inner vestibule (Fig. 9*A*), perhaps by physical withdrawal of hydrophobic amino acid side chains from the pore lumen.

Acknowledgments—We thank Dr. David Gadsby for providing cysless CFTR cDNA and Dr. Elizabeth Cowley for comments on the manuscript.

REFERENCES

1. Rowe, S. M., Miller, S., and Sorscher, E. J. (2005) *N. Engl. J. Med.* **352,** 1992–2001
2. Gadsby, D. C., Vergani, P., and Csanády, L. (2006) *Nature* **440,** 477–483
3. Pilewski, J. M., and Frizzell, R. A. (1999) *Physiol. Rev.* **79,** S215–S255
4. Poulsen, J. H., Fischer, H., Illek, B., and Machen, T. E. (1994) *Proc. Natl. Acad. Sci. U.S.A.* **91,** 5340–5344
5. Hug, M. J., Tamada, T., and Bridges, R. J. (2003) *News Physiol. Sci.* **18,** 38–42
6. Tang, L., Fatehi, M., and Linsdell, P. (2009) *J. Cyst. Fibros.* **8,** 115–121
7. Linsdell, P., and Hanrahan, J. W. (1998) *Am. J. Physiol.* **275,** C323–C326
8. Xu, Y., Szép, S., and Lu, Z. (2009) *Proc. Natl. Acad. Sci. U.S.A.* **106,** 20515–20519
9. McCarty, N. A. (2000) *J. Exp. Biol.* **203,** 1947–1962
10. Linsdell, P. (2006) *Exp. Physiol.* **91,** 123–129
11. St. Aubin, C. N., and Linsdell, P. (2006) *J. Gen. Physiol.* **128,** 535–545
12. Fatehi, M., and Linsdell, P. (2009) *J. Membr. Biol.* **228,** 151–164
13. Zhou, J. J., Li, M. S., Qi., J., and Linsdell, P. (2010) *J. Gen. Physiol.* **135,** 229–245
14. Hwang, T. C., and Sheppard, D. N. (2009) *J. Physiol.* **587,** 2151–2161
15. Muallem, D., and Vergani, P. (2009) *Philos. Trans. R. Soc. Lond. B Biol. Sci.* **364,** 247–255
16. Csanády, L., Vergani, P., and Gadsby, D. C. (2010) *Proc. Natl. Acad. Sci. U.S.A.* **107,** 1241–1246
17. Mense, M., Vergani, P., White, D. M., Altberg, G., Nairn, A. C., and Gadsby, D. C. (2006) *EMBO J.* **25,** 4728–4739
18. Li, M. S., Demsey, A. F., Qi, J., and Linsdell, P. (2009) *Br. J. Pharmacol.* **157,** 1065–1071
19. Gong, X., Burbridge, S. M., Cowley, E. A., and Linsdell, P. (2002) *J. Physiol.* **540,** 39–47
20. Linsdell, P., and Hanrahan, J. W. (1996) *J. Physiol.* **496,** 687–693
21. Linsdell, P., and Gong, X. (2002) *J. Physiol.* **540,** 29–38
22. Linsdell, P., and Hanrahan, J. W. (1998) *J. Gen. Physiol.* **111,** 601–614
23. Gong, X., and Linsdell, P. (2003) *J. Gen. Physiol.* **122,** 673–687
24. Mornon, J. P., Lehn, P., and Callebaut, I. (2008) *Cell. Mol. Life Sci.* **65,** 2594–2612
25. Akabas, M. H., Kaufmann, C., Cook, T. A., and Archdeacon, P. (1994) *J. Biol. Chem.* **269,** 14865–14868
26. Smith, S. S., Liu, X., Zhang, Z. R., Sun, F., Kriewall, T. E., McCarty, N. A., and Dawson, D. C. (2001) *J. Gen. Physiol.* **118,** 407–431
27. Zhang, Z. R., Song, B., and McCarty, N. A. (2005) *J. Biol. Chem.* **280,** 41997–42003
28. Beck, E. J., Yang, Y., Yaemsiri, S., and Raghuram, V. (2008) *J. Biol. Chem.* **283,** 4957–4966
29. Fatehi, M., and Linsdell, P. (2008) *J. Biol. Chem.* **283,** 6102–6109
30. Alexander, C., Ivetac, A., Liu, X., Norimatsu, Y., Serrano, J. R., Landstrom, A., Sansom, M., and Dawson, D. C. (2009) *Biochemistry* **48,** 10078–10088
31. Cheung, M., and Akabas, M. H. (1996) *Biophys. J.* **70,** 2688–2695
32. Serrano, J. R., Liu, X., Borg, E. R., Alexander, C. S., Shaw, C. F., 3rd, and Dawson, D. C. (2006) *Biophys. J.* **91,** 1737–1748
33. Serohijos, A. W., Hegedus, T., Aleksandrov, A. A., He, L., Cui, L., Dokholyan, N. V., and Riordan, J. R. (2008) *Proc. Natl. Acad. Sci. U.S.A.* **105,** 3256–3261
34. Mornon, J. P., Lehn, P., and Callebaut, I. (2009) *Cell. Mol. Life Sci.* **66,** 3469–3486
35. Liu, X., Zhang, Z. R., Fuller, M. D., Billingsley, J., McCarty, N. A., and Dawson, D. C. (2004) *Biophys. J.* **87,** 3826–3841
36. Cotten, J. F., and Welsh, M. J. (1999) *J. Biol. Chem.* **274,** 5429–5435
37. Cui, G., Zhang, Z. R., O'Brien, A. R., Song, B., and McCarty, N. A. (2008) *J. Membr. Biol.* **222,** 91–106
38. Jordan, I. K., Kota, K. C., Cui, G., Thompson, C. H., and McCarty, N. A. (2008) *Proc. Natl. Acad. Sci. U.S.A.* **105,** 18865–18870
39. Cui, L., Aleksandrov, L., Hou, Y. X., Gentzsch, M., Chen, J. H., Riordan, J. R., and Aleksandrov, A. A. (2006) *J. Physiol.* **572,** 347–358
40. Wang, Y., Loo, T. W., Bartlett, M. C., and Clarke, D. M. (2007) *J. Biol. Chem.* **282,** 33247–33251
41. Ge, N., Muise, C. N., Gong, X., and Linsdell, P. (2004) *J. Biol. Chem.* **279,** 55283–55289
42. Csanády, L., Nairn, A. C., and Gadsby, D. C. (2006) *J. Gen. Physiol.* **128,** 523–533
43. Scott-Ward, T. S., Cai, Z., Dawson, E. S., Doherty, A., Da Paula, A. C., Davidson, H., Porteous, D. J., Wainwright, B. J., Amaral, M. D., Sheppard, D. N., and Boyd, A. C. (2007) *Proc. Natl. Acad. Sci. U.S.A.* **104,** 16365–16370
44. Rosenberg, M. F., Kamis, A. B., Aleksandrov, L. A., Ford, R. C., and Riordan, J. R. (2004) *J. Biol. Chem.* **279,** 39051–39057
45. Zhang, L., Aleksandrov, L. A., Zhao, Z., Birtley, J. R., Riordan, J. R., and Ford, R. C. (2009) *J. Struct. Biol.* **167,** 242–251
46. Kos, V., and Ford, R. C. (2009) *Cell. Mol. Life Sci.* **66,** 3111–3126
47. Locher, K. P. (2009) *Philos. Trans. R. Soc. Lond. B Biol. Sci.* **364,** 239–245

48. Gadsby, D. C. (2009) *Nat. Rev. Mol. Cell Biol.* **10,** 344–352
49. Miller, C. (2010) *Proc. Natl. Acad. Sci. U.S.A.* **107,** 959–960
50. Doyle, D. A., Morais, Cabral, J., Pfuetzner, R. A., Kuo, A., Gulbis, J. M., Cohen, S. L., Chait, B. T., and MacKinnon, R. (1998) *Science* **280,** 69–77
51. Jiang, Y., Lee, A., Chen, J., Cadene, M., Chait, B. T., and MacKinnon, R. (2002) *Nature* **417,** 523–526
52. Long, S. B., Campbell, E. B., and Mackinnon, R. (2005) *Science* **309,** 897–903
53. Tao, X., Avalos, J. L., Chen, J., and MacKinnon, R. (2009) *Science* **326,** 1668–1674
54. Unwin, N. (2005) *J. Mol. Biol.* **346,** 967–989
55. Kawate, T., Michel, J. C., Birdsong, W. T., and Gouaux, E. (2009) *Nature* **460,** 592–598
56. Miller, C. (2006) *Nature* **440,** 484–489
57. Li, H., and Sheppard, D. N. (2009) *BioDrugs* **23,** 203–216
58. Linsdell, P. (2005) *J. Biol. Chem.* **280,** 8945–8950
59. St. Aubin, C. N., Zhou, J. J., and Linsdell, P. (2007) *Mol. Pharmacol.* **71,** 1360–1368